Comparing the recovery of rare earth elements from ion-adsorption clay leach solutions using various precipitants

by J. Chivavava[1], J. Petersen[2], and A.E. Lewis[1]

Affiliation:
[1]Crystallization and Precipitation Unit, Department of Chemical Engineering, University of Cape Town, South Africa
[2]Hydrometallurgy Research Group, Department of Chemical Engineering, University of Cape Town, South Africa

Correspondence to:
J. Chivavava

Email:
jemitias.chivavava@uct.ac.za

Dates:
Received: 23 Aug. 2024
Published: December 2024

How to cite:
Chivavava, J., Petersen, J., and Lewis, A.E. 2024. Comparing the recovery of rare earth elements from ion-adsorption clay leach solutions using various precipitants. *Journal of the Southern African Institute of Mining and Metallurgy*, vol. 124, no.12 pp. 737–746

DOI:
http://dx.doi.org/10.17159/2411-9717/730/2024

ORCID:
J. Chivavava
http://orcid.org/0000-0002-4640-9640
J. Petersen
http://orcid.org/0000-0003-2976-308X
A.E. Lewis
http://orcid.org/0000-0001-6544-1227

This paper is based on a presentation given at the Hydrometallurgy Conference 2024, 1-3 September 2024, Hazendal Wine Estate, Stellenbosch, Western Cape, South Africa

Abstract

Rare earth elements (REEs) have special properties that prompted their extensive use in high-tech applications. The demand for REE has, therefore, increased over the past years, resulting in the supply risk of the materials. Extraction from non-conventional low-grade ores, like easy-to-mine ion-adsorption clays (IACs), by hydrometallurgical methods is being explored to supplement the supply of REEs. The extraction of REEs from low tenor IAC leach solutions requires enrichment using cost-effective methods such as precipitation. Therefore, the aim of this study was to understand the recovery of REEs from IAC leach solutions using various reagents for precipitation. In the first part of the study, recoveries of REEs from IAC leach solutions through direct precipitation using $H_2C_2O_4$ and NH_4HCO_3, as well as antisolvent crystallization using C_2H_5OH, were predicted via thermodynamic modelling using OLI Stream Analyzer. Verification experiments were then conducted through the use of an agitated reactor. Simulation results showed that high yields of REEs were possible using each of the reagents, but large quantities of C_2H_5OH were required. Experimental results confirmed the high yields predicted from simulations. Precipitation with $H_2C_2O_4$ was found to selectively recover REEs while rejecting Al. However, utilization of NH_4HCO_3 and C_2H_5OH resulted in the co-precipitation of Al. Furthermore, the yield of Y from antisolvent crystallization was significantly lower than the theoretical value. The product recovered from antisolvent crystallization consisted of well-faceted, large crystalline particles, which filtered faster than the fine, amorphous REE carbonates recovered using NH_4HCO_3. REE oxalates were crystalline, larger than the REE carbonates and, overall, showed the highest filtration rate.

Keywords

rare earth elements, antisolvent crystallization, precipitation, ion adsorption clays

Introduction

Rare earth elements (REEs) are 17 metallic elements consisting of 15 lanthanides, scandium, and yttrium. The materials have special physico-chemical properties due to their screened 4f electrons and have several applications in the electronics, renewable energy, automobile, telecommunication, aerospace and security industry (Xie et al., 2014). The demand for REEs has increased substantially over recent years due to new applications in the energy transition economy (Korkmaz et al., 2020). Furthermore, geo-political factors have resulted in the global supply risk of REEs such as Nd and Dy, which are regarded as critical materials in the USA and Europe (Grohol and Veeh, 2023). In order to avoid shortages in the supply of REEs, different economies have been implementing strategies such as circular economy, stockpiling, and diversification of REE sources (Salim et al., 2022).

Although production from high-grade primary ores such as bastnaesite (Ce,La,Nd)(CO_3)F, monazite (Ce,La,Nd)PO_4, xenotime (YPO_4), and loparite (Soltani et al., 2019; Wu et al., 2018) could be increased where the ores are available, the extraction of REEs from such ores is still faced with process and economic viability challenges. Harsh processing conditions and strict hazard management against radioactivity in the processing of monazite restricts its exploitation (Ahmed, 2017). Therefore, to supplement the current supply from conventional primary ores, there are attempts to recover REEs from spent products, tailings, and other non-conventional ores. However, the recycling of REEs from spent permanent magnets, nickel-metal hydride batteries, and catalysts can only partially resolve the supply risk of REEs. Thus, extraction of REEs from tailings like phosphogypsum and red mud, from the processing of phosphate minerals and bauxite, respectively, is necessary to secure and diversify the supply chains.

The supply of heavy REEs (HREEs), i.e., Sm (62) to Lu (71) and Y(39), remains insecure and even primary ores, such as bastnaesite, have low HREE content (Gupta and Krishnamurthy, 2005; Schulze et

al., 2017). Although ion-adsorption clays (IACs) have low grades of REEs, the ores are important sources of HREEs (Schulze et al., 2017). Thus, the extraction of REEs from IACs in China has contributed significantly to the global supply of HREEs. The recovery of REEs from IACs does not require extensive physical beneficiation, which offsets their low REE grades, making the extraction of REEs from such ores cost-effective (Huang et al., 2015; Xiao et al., 2015; Yin et al., 2020). Furthermore, IACs are less hazardous due to very low concentrations of radioactive Th and U (Schulze et al., 2017; Burcher-Jones et al., 2018). However, the mineralogy of IACs varies widely and the leaching of REEs from the ores results in dilute pregnant leach solutions (PLS) containing Fe, Al, Si, Ca, Na, Mg, NH_4^+, and SO_4^{2-} impurities (Chi and Tian, 2008; Schulze et al., 2017). Outside China, IAC ores have been found in several African countries and South America (Nyakairu and Koeberl, 2001; Burcher-Jones et al., 2018; Ram et al., 2019; Temga et al., 2021).

The extraction of REEs from IAC ores involves either excavation followed by heap leaching, or drilling of boreholes and in situ leaching using aqueous $(NH_4)_2SO_4$ or $MgSO_4$ as lixiviants. During leaching, the ion-exchangeable REE fraction is desorbed from the surfaces of clay particles into the aqueous phase and is replaced by cations (NH_4^+ or Mg^{2+}) from the lixiviants. This generates low-tenor PLS of REEs containing impurities such as Fe, Al, and Si, which, together with lixiviant species, influence the aqueous chemistry. Thus, selective extraction of REEs from such impurity-laden and low-tenor leach solutions is necessary to upgrade REEs before downstream separation and refining processes. Although ion exchange, solvent extraction, and adsorption can recover REEs from PLS, precipitation is conventionally used to extract REEs from IAC leach solutions because it is cost-effective and relatively simpler than other methods. Precipitation occurs when the concentration of sparingly soluble compounds from the chemical reaction between REEs and anions, such as hydroxides, fluorides, phosphates, oxalates, and carbonates, exceed their solubility. Thus, concentrates of REEs are produced from low-tenor leach solutions of IACs primarily through bulk precipitation. Typically, Fe^{3+} and Al^{3+} are rejected from the PLS via precipitation at pHs of ~3.5 and ~5, respectively, using alkalis such as NaOH, $Ca(OH)_2$, NH_3, and NH_4HCO_3 (Chi and Xu, 1999; Chi and Tian, 2008; Zhou et al., 2017; da Silva et al., 2018; Silva et al., 2019; Judge and Azimi, 2020).

REEs are conventionally recovered from IAC pregnant leach solutions via precipitation with oxalic acid ($H_2C_2O_4$) and ammonium bicarbonate (NH_4HCO_3)(Chi and Tian, 2008). Precipitation with $H_2C_2O_4$ occurs at acidic pH via the reaction in Equation [1] (Chi and Tian, 2008; Schulze et al., 2017):

$$2REE^{3+}_{(aq)} + 3H_2C_2O_{4(aq)} + xH_2O_{(l)} = REE_2(C_2O_4)_3.xH_2O_{(s)} + 6H^+_{(aq)} \quad [1]$$

The use of $H_2C_2O_4$ achieves selective precipitation of REEs from impurity-laden pregnant leach solutions in a single stage and produces large REE oxalate particles, which are easy to dewater (Chi and Tian, 2008). However, $H_2C_2O_4$ is expensive, forms complexes with impurity species and generates acidic wastewaters from the operations. These challenges motivated the adoption of NH_4HCO_3 for precipitation of REEs from PLS of IAC ores. This occurs at pH between 5 and 8, often after prior rejection of metal impurities at lower pH, and proceeds according to the reaction in Equation [2] (Chi and Tian, 2008; Anawati and Azimi, 2022);

$$2REE^{3+}_{(aq)} + 6NH_4HCO_{3(aq)} + xH_2O_{(l)} = REE_2(CO_3)_3.xH_2O_{(s)} + 3H_2O_{(l)} + 3CO_{2(g)} + 6NH_4^+{}_{(aq)} \quad [2]$$

NH_4HCO_3 is cheaper, relatively safer, neutralizes leach solutions, and replenishes $(NH_4)_2SO_4$ for recycling of the supernatant back to the leaching stage as a lixiviant. Furthermore, REE carbonates can be easily redissolved in acids for further processing. However, REE carbonates precipitate as fine amorphous particles, which are voluminous and difficult to dewater (Yin et al., 2020; Yu et al., 2020; Wang et al., 2021).

Recently, studies have shown that antisolvent crystallization can recover REEs from pregnant leach solutions of spent products and bauxite residue, as salt crystals with tunable physical properties (Kaya et al., 2018; Korkmaz et al., 2020; Pawar et al., 2024). Unlike oxalates and carbonates, sulphates of REEs are moderately soluble in water (Cunningham et al., 2024). Therefore, in antisolvent crystallization, water-miscible organic compounds with low dielectric constants reduce the solubility of dissolved REE salts in the resultant solution and induce crystallization of the salts when supersaturation is attained (Pawar et al., 2024). While high yields and recycling of antisolvents are possible, antisolvent crystallization is still being developed for industrial application in the recovery of metals. The method has been applied for the recovery of REEs from leach solutions with moderate tenors of REEs (Korkmaz et al., 2020), but has not been utilized for direct recovery of REEs from low tenor solutions, such as PLS' of IACs.

Overall, the recovery of REEs as carbonates is commonly practised and $H_2C_2O_4$ is still applied for the recovery of REEs where high purity is required, while antisolvent crystallization has shown huge potential as an alternative method of recovering REEs (Schulze et al., 2017; da Silva et al., 2018). $H_2C_2O_4$ and NH_4HCO_3 have different properties, react with REEs and impurity species differently, and produce particles with different physico-chemical characteristics resulting in process flowsheets with different levels of complexity. Antisolvents have different properties and their mechanism of action, i.e., polarization and dehydration of solutes, differs from that of classical precipitants (Korkmaz et al., 2020). Furthermore, the reagent demands, and the nature of the residual effluents differ. These aspects and operating conditions can be determined via thermodynamic simulation of aqueous chemistry.

Thermodynamic modelling of aqueous chemistry to predict equilibria and determine yields of REEs from PLS has been conducted using software such as PHREEQC, Visual MinteQ, and OLI Stream Analyzer (Judge et al., 2023). OLI Stream Analyzer uses the Helgeson-Kirkham-Flower equation of state while Visual MinteQ uses the Debye-Huckel and Davies equations to predict activities of the solutes in aqueous solutions. The solubility of respective REE compounds ultimately influences their precipitation behaviour. It is noted that solubility product constants (K_{sp}) of individual REE carbonates range from $10^{-35.8}$ to 10^{-28} and the data vary widely amongst different studies (Firsching and Mohammadzadei, 1986; Runde et al., 1992; Spahiu and Bruno, 1995; Chi and Tian, 2008). REE oxalates are slightly more soluble than carbonates and their Ksps vary between 10^{-32} and 10^{-25} (Chi and Tian, 2008; Xiong, 2011; Josso et al., 2018). The solubilities of $Y_2(SO_4)_3.8H_2O$ in different H_2O alcohol mixtures have been measured by Sussens et al. (2024), while solubility of various REE sulphates in H_2O have been determined by Judge et al. (2023) and Moldoveanu et al. (2024).

The overall aim of this study was therefore to determine the recovery of REEs from PLS' of IACs using bulk precipitation and antisolvent crystallization. The objective of the investigation was to study and compare the performance of different precipitants and antisolvents in the enrichment of REEs from IAC leach solutions.

Methods and materials

The extraction of REEs from PLS of IACs using NH_4HCO_3, $H_2C_2O_4$, CH_3OH, and C_2H_5OH was studied. A PLS obtained from the leaching of an IAC ore from Madagascar using 0.5M $(NH_4)_2SO_4$ was used as the basis of synthetic PLS' used in the experimental tests.

Thermodynamic modelling

The recovery of REEs from the IAC leach solution using precipitation was simulated using OLI Stream Analyzer to predict the yields of REEs, quantities of reagents, and precipitation conditions. The mixed solvent electrolyte (MSE) framework was used and extraction of REEs from the PLS using $H_2C_2O_4$, NH_4HCO_3, CH_3OH, and C_2H_5OH was simulated. Although thermodynamic data and models were available for a very limited number of REE carbonates and oxalates in OLI Stream Analyzer, the software was selected for simulations because it contained thermodynamic data and models for REE sulphates (Nd, Y, and Dy) in the C_2H_5OH-H_2O system. The models were developed by OLI Systems Inc. for the University of Cape Town and included $Y_2(SO_4)_3$ in the CH_3OH-H_2O system (Sussens et al., 2024). The software contained thermodynamic data and models for Nd carbonate and oxalate, as well as Yb oxalate. Thermodynamic data and a model for $Dy_2(CO_3)_3$ in water were developed by OLI Systems Inc. for the University of Cape Town as part of this study. Although Visual MinteQ and PHREEQC databases contain thermodynamic data for several carbonates and oxalates, OLI Stream Analyzer was used for all simulations in this study for consistency.

The recovery of Nd from 1 L of the IAC leach solution containing 433 ppm of Nd^{3+} and 300 ppm of Al^{3+} in aqueous $(NH_4)_2SO_4$ solution using precipitation/crystallization with $H_2C_2O_4$, NH_4HCO_3, and C_2H_5OH was simulated. The crystallization of $Y_2(SO_4)_3$ from the same aqueous matrix using CH_3OH and C_2H_5OH was also simulated since its thermodynamic data and models in both systems were available.

Laboratory experimental tests

Laboratory experiments were carried out to compare the recovery of REEs from IAC leach solutions using $H_2C_2O_4$, NH_4HCO_3, CH_3OH, and C_2H_5OH. Although preliminary experiments were conducted using the PLS obtained from the leaching of IAC ore from Madagascar, the quantity of the solution was limited, hence simplified, synthetic leach solutions were prepared and used for further investigations. The simplified model PLS' contained only major REEs, Al^{3+}, and lixiviant species as shown in Table I.

Reagent grade $La_2(SO_4)_3$, $Pr_2(SO_4)_3.8H_2O$, $Nd_2(SO_4)_3.8H_2O$, $Y_2(SO_4)_3.8H_2O$ (ThermoFisher, Germany), $(NH_4)_2SO_4$ (Merck, South Africa), and $Al_2(SO_4)_3.xH_2O$ (Sigma-Aldrich, South Africa) were dissolved in deionized water to prepare synthetic PLS'. Precipitant aqueous solutions were prepared by dissolving 4.3 g of $H_2C_2O_4$ (Sigma Aldrich) and 10 g of NH_4HCO_3 (Merck and Sigma Aldrich) in 1 L of deionized water, but both CH_3OH and C_2H_5OH (Kimix, South Africa) were utilized without modification.

Laboratory tests were conducted to determine the yields of REEs when each of the four reagents was used, separately, to recover REEs from the IAC leach solution. In the experiments, 200 mL of 0.43 wt.% $H_2C_2O_4$ and 1 wt.% NH_4HCO_3 aqueous solutions were individually added to 200 mL of synthetic PLS to precipitate REE oxalates and carbonates, respectively. In order to crystallize REE sulphates, 171 mL of C_2H_5OH and 200 mL of CH_3OH were added to 200 mL of synthetic PLS in different experiments. These resulted in organic to aqueous (O/A) ratios of 0.86 for C_2H_5OH and 1.0 for CH_3OH, which were selected to avoid co-crystallization of $(NH_4)_2SO_4$ while achieving theoretical yields of total rare earth elements (TREEs) higher than 95%. In a separate experiment (AS3), the C_2H_5OH quantity was increased to 230 mL in an attempt to improve the recovery of REEs. A summary of the experiments is provided in Table II.

Experimental equipment

All experimental tests were conducted using an agitated 0.5 L glass reactor, fitted with three baffles, as illustrated in Figure 1. An overhead stirrer (IKA RW20), connected to a 6-blade Rushton turbine (0.033 m), was used for agitation and a Mettler Toledo pH electrode was used to measure the pH of the reactor contents. A peristaltic pump (Watson Marlow, 520S) was used to add precipitants and antisolvents into the reactor.

Experimental procedure

Two hundred (200) mL of the PLS was initially added into the reactor and the agitator was started. The precipitant/antisolvent was then pumped into the reactor using a peristaltic pump. In the case of C_2H_5OH, 171 mL and 230 mL were added to 200 mL and 181 mL

Table I

Concentrations of REEs, Al^{3+}, NH_4^+ and SO_4^{2-} in the model PLS

Species	La^{3+}	Nd^{3+}	Pr^{3+}	Y^{3+}	Al^{3+}	NH_4^+	SO_4^{2-}
Concentration(mg/L)	800	433	137	240	300	13 830	40 239

Table II

Details of conducted experiments and utilized reagents

Exp.	Reagent	Conc. (g/L)/ purity (%) *	Volume of reagent(mL)	Volume of PLS (mL)	O/A(v/v)
R1	$H_2C_2O_4$	4.3	200	200	–
R2	NH_4HCO_3	10	200	200	–
AS1	CH_3OH*	99.8	200	200	1.0
AS2	C_2H_5OH*	99.9	171	200	0.86
AS3	C_2H_5OH*	99.9	230	181	1.3

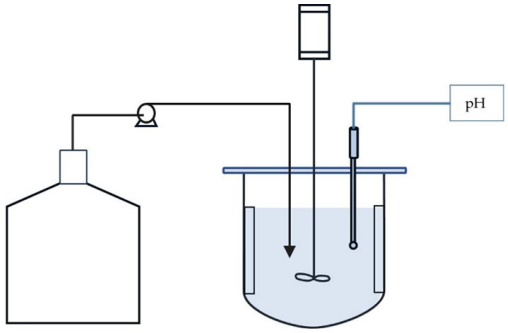

Figure 1—Reagent bottle, peristaltic pump, overhead stirrer and 0.5 L reactor

of PLS, respectively. The agitator rotational speed was 500 rpm, and this was selected to avoid the settling of product particles during antisolvent crystallization. Each experiment was run for 2 hours to allow time for antisolvent crystallization of REEs, which was relatively slower at the selected O/A ratios, while keeping the duration relatively shorter to suit industrial operations (Silva et al., 2019). All experiments were repeated at least twice.

After each experiment, samples of the slurry were collected for size analysis using laser diffraction (Malvern Mastersizer 2000, UK). The remainder of the product slurry was harvested and vacuum-filtered using 0.22 µm nylon membrane filters, Merck Millipore flask and funnel, as well as an oil-less piston vacuum pump (Vacutec, South Africa). The filtration was monitored to determine the performance of the different products. Samples of the filtrate were collected for metal analysis, using inductively coupled plasma mass spectrometry (ICP-MS) (Agilent 7900, USA), to quantify the yields of REEs. The yields were estimated from Equation [3]:

$$\text{Yield of REE} = \frac{C_o V_o - C_s V_s}{C_o V_o} \times 100\% \quad [3]$$

C_o and Cs are concentrations of the metal ions in the PLS and in the supernatant (ppm), respectively; V_o and V_s are the respective volumes (mL). After drying in the desiccator for at least 24 hours, samples of the products were collected for imaging and elemental analysis using the scanning electron microscope (Tescan Mira 3 RISE, Czech Republic) and energy dispersive X-ray spectroscopy (EDS). Samples of products from antisolvent crystallization were also analysed using powder X-ray diffraction (XRD).

Results and discussion

Thermodynamic Modelling: Recovery of Nd from an IAC leach solution using different reagents

The recovery of Nd from 1 L of the simplified IAC pregnant leach solution using $H_2C_2O_4$, NH_4HCO_3 and C_2H_5OH was simulated using OLI Stream Analyzer (see Figure 2). The results showed that, further to conventional precipitation using $H_2C_2O_4$ and NH_4HCO_3, antisolvent crystallization using C_2H_5OH can recover high yields of REEs from IAC leach solutions. The recovery of Nd using CH_3OH could not be modelled because thermodynamic data for the $Nd_2(SO_4)_3$-H_2O-CH_3OH system was unavailable at this stage. The yields of Nd from the IAC leach solution containing 433 ppm of Nd^{3+} are shown in Figure 2 as a function of the amounts of reagents utilized for recovery.

It was predicted that the amount of $H_2C_2O_4$ required to recover >90% of Nd from 1 L of PLS was the least, but comparable to that of NH_4HCO_3, while the amount of C_2H_5OH required to recover the same amount of Nd was almost two orders of magnitude higher. The marked difference in the reagent demand can be attributed to the differences in the mechanisms of action of the reagents and solubility behaviour of the recovered products.

While $H_2C_2O_4$ and NH_4HCO_3 provide $C_2O_4^{2-}$ and HCO_3^- anions for reactive precipitation of $Nd_2(C_2O_4)_3.10H_2O$ and $NdOHCO_3$, respectively, C_2H_5OH induces the crystallization of $Nd_2(SO_4)_3.8H_2O$ via a different mechanism. C_2H_5OH reduces both the activity of water and the dielectric constant of the solution, which dehydrates and reduces polarization of the ions, respectively, thus facilitating the crystallization of REE sulphates (Korkmaz et al., 2020). It is noted that $NdOHCO_3$, which is more soluble than $Nd_2(CO_3)_3$, was predicted as the thermodynamically stable phase. $Nd_2(SO_4)_3.8H_2O$, was predicted to crystallize from the $Nd_2(SO_4)_3$-H_2O-C_2H_5OH system and this was confirmed experimentally through XRD analysis by Pawar et al. (2024). The same compound was found to be the stable phase that crystallizes from $Nd_2(SO_4)_3$-H_2O solutions at room temperature (Das et al., 2019; Judge et al., 2023; Moldoveanu et al., 2024).

Al^{3+} was predicted to remain in the aqueous phase when $H_2C_2O_4$ was used to precipitate REEs from the IAC leach solution. This is due to the formation of soluble Al oxalate complexes, such as $AlH_3[C_2O_4]_2^{2+}$, which remain in aqueous phase as REE oxalates precipitate. Contrary to this, the utilization of NH_4HCO_3 was predicted to co-precipitate $Al(OH)_3$ and $Nd(OH)CO_3$. However, the $Al(OH)_3$ was predicted to precipitate at a lower pH than $Nd(OH)CO_3$, thus presenting an opportunity for sequential precipitation (Chi et al., 2003). Lastly, it was predicted that adding more than 670 g of C_2H_5OH to 1 L of PLS would result in the co-precipitation of $(NH_4)_2SO_4$ with $Nd_2(SO_4)_3.8H_2O$. Operationally, the crystallization of the lixiviant limits the amount of antisolvent that can be utilized, although the antisolvent can be recovered.

Experimental: Precipitation of REEs from PLS of IACs using different reagents

Yields of REEs and rejection of Al by different precipitants/antisolvents

The yields of the metals were evaluated using Equation [3] and the residual metal content in the supernatants, with results presented in Figure 3. The yields of TREEs were generally high when each of the four reagents was used to recover REEs from synthetic IAC leach solutions.

The highest recovery of TREEs (>99%) was achieved by using 1 wt.% NH_4HCO_3 aqueous solution for bulk precipitation and a similar yield (>98%) was achieved by using 0.43 wt.% $H_2C_2O_4$ aqueous solution. Crystallization of REEs using CH_3OH(OA=1) resulted in a 92% yield of TREEs, while crystallization using C_2H_5OH, at O/A=0.86 and 1.27, recovered 88% and 93%,

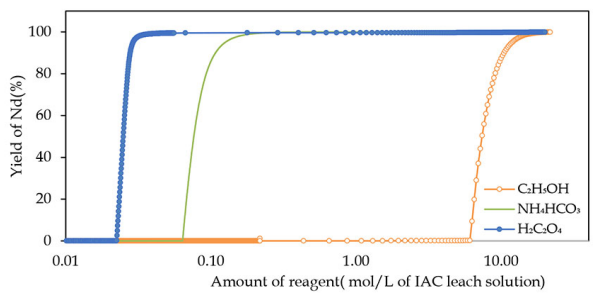

Figure 2—Recoveries of Nd from IAC leachate using $H_2C_2O_4$, NH_4HCO_3, and C_2H_5OH

respectively. As shown in Figure 3, Al was virtually rejected when $H_2C_2O_4$ was utilized to recover REEs from the IAC leach solutions, but was co-extracted with REEs when NH_4HCO_3, CH_3OH and C_2H_5OH were used to precipitate REEs in a single stage. Although CH_3OH rejected Al slightly better than C_2H_5OH (O/A=0.86) during crystallization of REE sulphates from IAC leach solutions, both antisolvents were less selective at the conditions employed in this study. The higher rejection of Al by CH_3OH was probably due to its higher dielectric constant than that of C_2H_5OH (Korkmaz et al., 2020; Sussens et al., 2024).

The high yields of TREEs obtained from precipitation using NH_4HCO_3 and $H_2C_2O_4$ were expected due to the extremely low solubilities of REE carbonates and oxalates, which resulted in high supersaturations and fast precipitation of REEs (Firsching and Mohammadzadei, 1986; Chi and Tian, 2008; Josso et al., 2018). Thus, instantaneous formation of particles occurred upon addition of the precipitants during experiments. The individual yields of La, Pr, and Nd recovered using CH_3OH(O/A=1) and C_2H_5OH, at both O/A= 0.86 and 1.27, were generally high (>96%) and similar for all the reagents after 2 hours of crystallization. Therefore, the relatively lower yields of TREEs obtained in antisolvent crystallization were attributed to the yields of Y, which was significantly lower than the rest of the REEs, as demonstrated in Figure 4. The lower yield suggests that the crystallization of Y using C_2H_5OH at O/A=0.86 was slower than that of other REEs.

Increasing the amount of C_2H_5OH to O/A=1.27 and utilizing CH_3OH(O/A=1) for crystallization enhanced the yield of Y significantly, but the recovery still remained below the theoretical values predicted from thermodynamic simulation, as demonstrated in Figure 5. The slow crystallization of Y could not be explained fully, but the behaviour could be attributed to the solubility of $Y_2(SO_4)_3.8H_2O$, which is higher than that of light REEs and similar to other HREEs. Analysis of the scaling tendency (S) using OLI Stream Analyzer showed that the supersaturation of $Y_2(SO_4)_3.8H_2O$ (S=555) was significantly lower than that of $Nd_2(SO_4)_3.8H_2O$ (S=3010) at C_2H_5OH (O/A=0.86). This possibly explains the associated slower crystallization kinetics at O/A=0.86, as shown

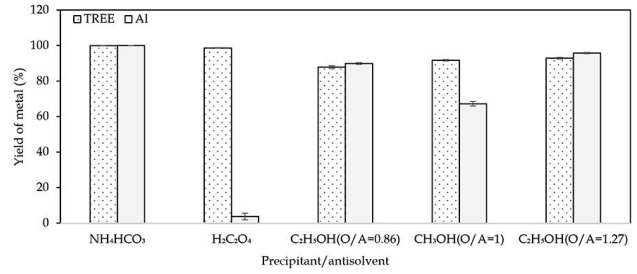

Figure 3—Yields of TREEs and Al for different precipitants after 2 h of precipitation/crystallization

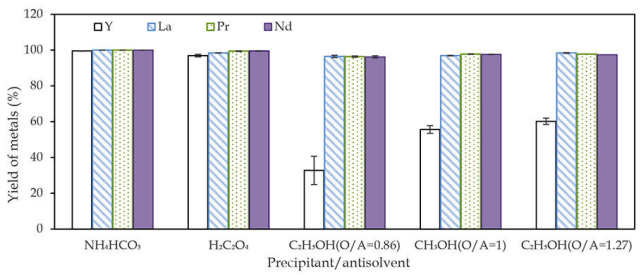

Figure 4—Yields of REES from the IAC leach solution for different precipitants after a batch time of 2 h

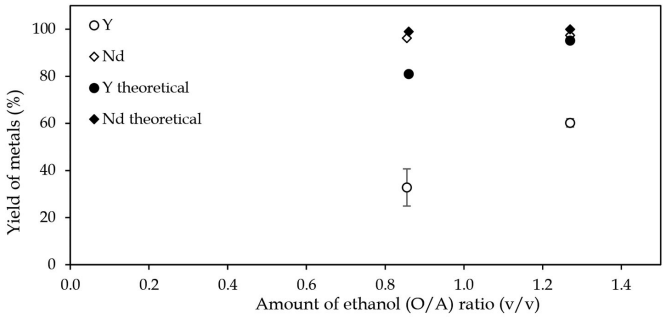

Figure 5—Experimental versus theoretical yields of Nd and Y after 2 h of crystallization at O/A(v/v) of 0.86 and 1.27

by lower yields. Although increasing the amount of C_2H_5OH to O/A=1.27 enhanced the supersaturation of the anhydrous $Y_2(SO_4)_3$ by two orders of magnitude, S=6.5x10⁴, the Y yield remained significantly lower than the theoretical value. The slow crystallization of Y was also observed by Korkmaz et al. (2020) in the recovery of REEs from leach solutions of NiMH batteries. Further studies to understand the crystallization behaviour of $Y_2(SO_4)_3$ during antisolvent crystallization are recommended.

The selective precipitation of REEs from IAC leach solution achieved using 0.43 wt.% $H_2C_2O_4$ aqueous solution was attributed to the formation of the soluble $AlH_3[C_2O_4]_2^{2+}$ complex at acidic pH, which remained in the aqueous phase during precipitation of REE oxalates, as suggested by thermodynamic simulation results (OLI Systems Inc, 2021). Elemental analysis of the REE oxalates product using EDS affirmed the rejection of Al during precipitation, as demonstrated in Figure 6a. The small amount of Al shown in Figure 3 was attributed to adsorption, which was also low. The high Al rejection efficiency in the recovery of REEs using $H_2C_2O_4$ was also reported by Silva et al. (2019).

The least rejection of Al observed using NH_4HCO_3 was due to co-precipitation of $Al(OH)_3$ with REE carbonates. This lowered the purity of the REE concentrates and was predicted from thermodynamic simulation. The comparably low rejection of Al achieved during crystallization of REE sulphates from IAC leach solution using C_2H_5OH and CH_3OH was attributed to co-crystallization of Al. This was supported by EDS of the product recovered using CH_3OH, which showed that the darker phase in Figure 6b (trigonal pyramid particles) contained Al. This was not predicted from simulation of aqueous chemistry and the identity of the Al compound that co-crystallized with REE sulphates during crystallization with both CH_3OH and C_2H_5OH could not be established at this stage, as XRD analysis of the product was still inconclusive. However, the crystallization of an Al sulphate salt during antisolvent crystallization with C_2H_5OH is possible and has been reported by Kang et al. (1995). Ma et al. (2023) further showed that Al co-crystallized during antisolvent crystallization of metals from PLS of Li-ion batteries.

Qualitative observations on filtration performance of products

The filtration performance of the products generated using the different reagents was monitored and filtration rates are presented in Figure 7.

REE oxalates filtered at the fastest rate while REE carbonates filtered at the slowest rate. The filter cake of the REE carbonates also developed micro- and macro-fissures during filtration, which showed poor dewatering behaviour. The filtration of the product recovered using CH_3OH(O/A=1) was faster, but comparable to

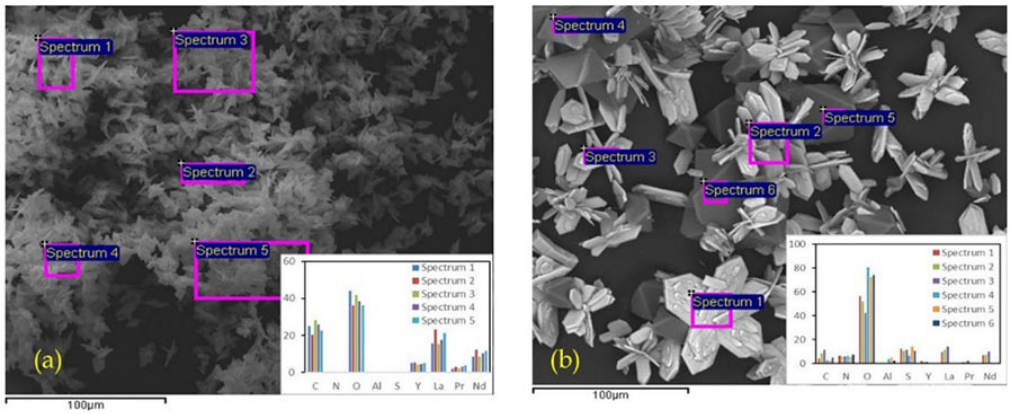

Figure 6—Energy dispersive X-ray spectroscopy (EDS) for REE oxalates from 0.43 wt.% $H_2C_2O_4$ and REE sulphates recovered using CH_3OH(O/A=1)

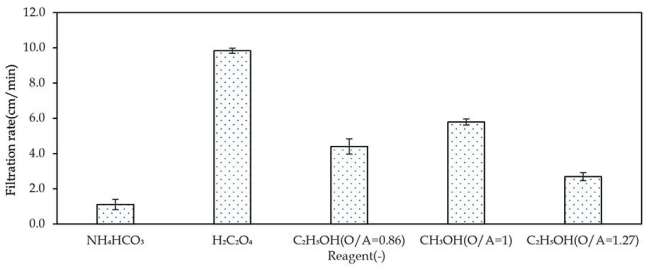

Figure 7—Filtration performance of the slurry produced using 0.43 wt.% $H_2C_2O_4$, 1 wt.% NH_4HCO_3, CH_3OH(O/A=1) and C_2H_5 OH(O/A=0.86&1.27) at N=500 rpm after 2h

that of the product recovered using C_2H_5OH(O/A=0.86). Utilising higher quantities of C_2H_5OH(O/A=1.27) produced a suspension that filtered at a slower rate. The difference in filtration performance was attributed to the differences in particle sizes, lattice structure, and habit of the products recovered using the different reagents. These properties determine the packing of the particles and the subsequent permeability of the filter cakes. Particle size distributions (PSDs) of the precipitates obtained from the experimental tests conducted for average batch times of 2 hours are shown in Figure 8.

The highest filtration rate of REE oxalates was attributed to crystalline particles, a narrow PSD and extensive particle clustering, which is evident in Figure 9(d-f). The crystalline prismatic particles had a mixture of sharp and rounded edges. On the contrary, the poor filterability of REE carbonates was due to both smaller particle sizes and amorphous structure. As shown in SEM micrographs in Figure 9 (a-c), small spherical and amorphous particles were produced when NH_4HCO_3 was utilized for precipitation. The fast filtration of the suspensions obtained using C_2H_5OH(O/A=0.86) and CH_3OH(O/A=1) can be attributed to the large, well-faceted, and predominantly crystalline product particles as shown in Figure 8 and Figure 9.

Although the product recovered using C_2H_5OH(O/A=0.86) consisted of slightly bigger particles than from CH_3OH(O/A=1), as presented in Figure 8, the product from the latter filtered slightly better, possibly due to lower viscosity of the residual CH_3OH-PLS solution. The product from crystallization using C_2H_5OH consisted of a mixture of prismatic and bipyramidal particles, with instances of sharp edges, broken corners, and intergrowth as illustrated in Figure 9(g-h). A phase with no clearly defined morphology was observed on the surfaces of bigger particles at higher magnifications (Figure 9i). Crystallization with CH_3OH produced a similar mixture of particle morphologies as shown in Figure 9(j-k). However, sheaves were also produced as shown in Figure 9j.

Although more than just REE compounds crystallized when NH_4HCO_3, CH_3OH, and C_2H_5OH were used to recover REEs, it was clear that crystal growth was dominant during antisolvent crystallization, hence the clearly defined product morphology. However, the poorly structured material that attached to the

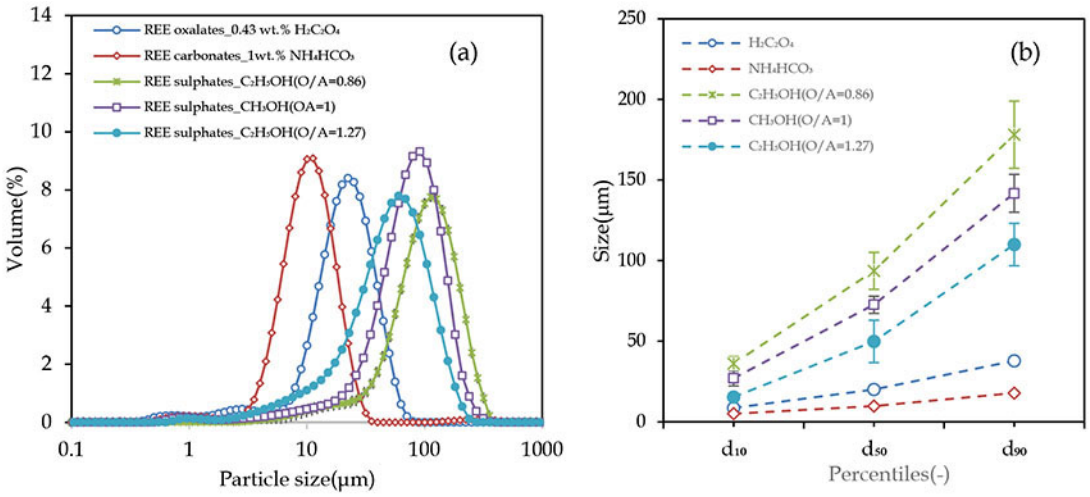

Figure 8—Particle size distribution (a) and mean particle sizes (b) of the REE precipitates obtained using different reagents after running each experiment for 2 h

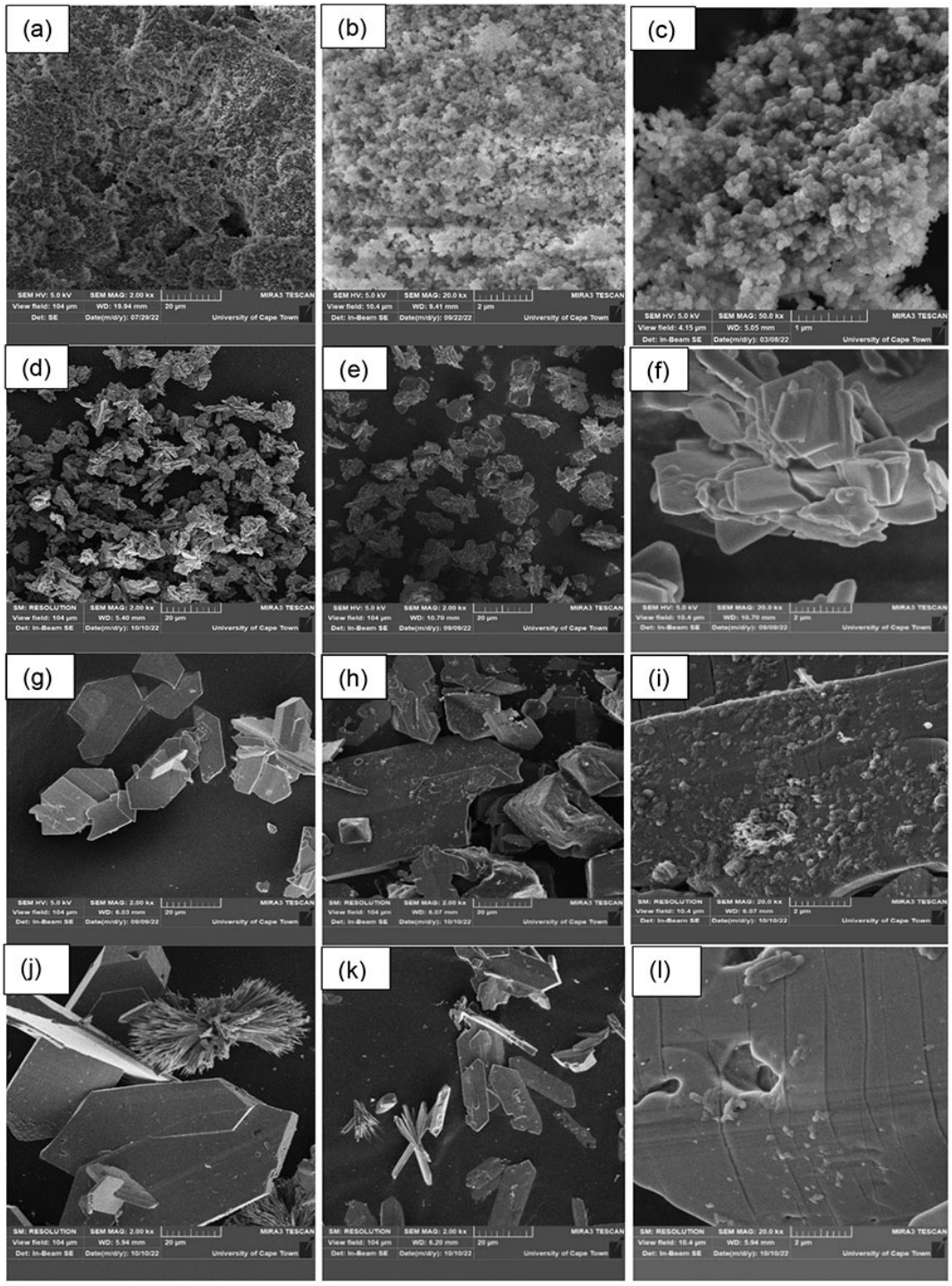

Figure 9—SEM micrographs of REE precipitates obtained from a synthetic IAC leach liquor using (a-c) 1 wt.% NH_4HCO_3 (d-f) 0.43 wt.% $H_2C_2O_4$ (g-i) C_2H_5OH(O/A=0.86) (j-l) CH_3OH (O/A=0.93)

surfaces of bigger particles suggests that the crystallization pathways were less obvious. An intensely white suspension formed after addition of the antisolvents, and this became progressively less with time. The formation of amorphous REE carbonates is extensively reported in previous studies and was therefore expected (Chi and Tian, 2008; Yin et al., 2020; Yu et al., 2020; Wang et al., 2021). Contrarily, crystalline REE oxalates formed at similar yields. Thus, the role of anions in the precipitation of REEs is clearly shown by the differences in the quality of the products recovered using the different reagents, in as much as antisolvent molecules and counter-ions influence the crystallization process.

Conclusions

The recovery of REEs from PLS of ion-adsorption clay ores was investigated in this study to understand the technical efficacy of each reagent to enrich the REEs from low-tenor solutions. Thermodynamic simulation was conducted using OLI Stream Analyzer and it revealed that high yields of REEs could be achieved with reactive precipitation using either $H_2C_2O_4$ or NH_4HCO_3 and antisolvent crystallization with either CH_3OH or C_2H_5OH. The highest yields were obtained from precipitation using $H_2C_2O_4$ and NH_4HCO_3, but significantly large quantities of CH_3OH and C_2H_5OH were necessary to achieve similar yields.

Experimental results confirmed the high REE yields predicted from thermodynamic simulations, especially for $H_2C_2O_4$ and NH_4HCO_3. However, the recovery of Y from crystallization using both alcohols was significantly lower than the rest of the REEs and was below the thermodynamically predicted yield.

The utilization of NH_4HCO_3, CH_3OH and C_2H_5OH for single-stage crystallization resulted in the co-precipitation of Al, which was predicted in the use of NH_4HCO_3, but not in the case of alcohols. This meant that REE concentrates of low purity were recovered when each of these three reagents was utilized.

The utilization of $H_2C_2O_4$ in a single stage resulted in selective recovery of REEs (La, Nd, Pr, and Y), while Al remained in the spent solution, and resulted in a product with the best dewatering performance, i.e., highest filtration rate among the tested reagents. The product was crystalline and slightly larger than REE carbonates. Interestingly, the product recovered using alcohols was characterized by mostly well-faceted, large prismatic and crystalline particles that dewatered quite easily, as shown by good filtration performance. Thus, crystal growth appeared to be dominant in antisolvent crystallization of REEs at the O/A ratios employed in this study, as shown by the well-formed large and crystalline particles. The fine, amorphous product recovered using NH_4HCO_3 filtered at the slowest rate, and the process appeared to be dominated by nucleation and agglomeration.

Overall, it was concluded that the utilization of $H_2C_2O_4$ as a precipitant achieved the best results in a single stage compared to other reagents. However, the precipitation/crystallization conditions for other reagents were not optimized and this conclusion is based on the technical performance in a single precipitation stage. Consideration of economic, environmental safety and other external factors is necessary to further compare the reagents and guide the selection of suitable precipitants.

Acknowledgements

The authors would like to thank Mr Eddy Miiro for generating PLS' used in preliminary experiments, Ms Miranda Waldron of the Electron Microscope Unit for imaging services, colleagues in the Analytical Laboratory at the University of Cape Town and Ms Charney Anderson-Small of the Central Analytical Facilities at Stellenbosch for the analytical work.

References

Ahmed, U.A.Q. 2017. *A Hydrometallurgical Comparison between the Caustic and Sulphuric Acid Cracking of Steenkampskraal (SKK) Monazite*. MSc University of Cape Town.

Anawati, J., Azimi, G. 2022. Separation of rare earth elements from a South American ionic clay lixivium by sequential precipitation. *Hydrometallurgy*, 213, 105946.

Burcher-Jones, C., Mkhize, S., Becker, M., Ram, R., Petersen, J. Study of the deportment of REEs in ion adsorption clays towards the development of an in situ leaching strategy. *Extraction 2018: Proceedings of the First Global Conference on Extractive Metallurgy*, 2018. Springer, pp. 2429–2439.

Chi, R.A., Xu, Z.G. 1999. A solution chemistry approach to the study of rare earth element precipitation by oxalic acid. *Metallurgical and Materials Transactions B*, vol. 30, pp. 189–195.

Chi, R.A., Zhou, Z., Xu, Z., Hu, Y., Zhu, G., Xu, S. 2003. Solution-chemistry analysis of ammonium bicarbonate consumption in rare-earth-element precipitation. *Metallurgical and Materials Transactions B*, vol. 34, pp. 611–617.

Chi, R., Tian, J. 2008. *Weathered crust elution-deposited rare earth ores*, Nova Science Publishers.

Cunningham, S., Etherington-Rivas, M., Azimi, G. 2024. Solubility of neodymium and dysprosium sulfates at different pH and temperature and the effect of yttrium sulfate, sodium sulfate, and ammonium sulfate mixtures: Strengthening the predictive capacities of the OLI software. *Hydrometallurgy*, vol. 224, 106253.

Da Silva, R.G., De Morais, C.A., Teixeira, L.V., De Oliveira, É.D. 2018. Selective removal of impurities from rare earth sulphuric liquor using different reagents. *Minerals Engineering*, vol. 127, pp. 238–246.

Das, G., Lencka, M.M., Eslamimanesh, A., Wang, P., Anderko, A., Riman, R.E., Navrotsky, A. 2019. Rare earth sulfates in aqueous systems: Thermodynamic modeling of binary and multicomponent systems over wide concentration and temperature ranges. *The Journal of Chemical Thermodynamics*, vol. 131, pp. 49–79.

Firsching, F.H., Mohammadzadei, J. 1986. Solubility products of the rare-earth carbonates. *Journal of Chemical and Engineering Data*, vol. 31, pp. 40–42.

Grohol, M., Veeh, C. 2023. European Commission, Study on the Critical Raw Materials for the EU 2023 – Final Report. Brussels: DG Grow, European Commission.

Gupta, C., Krishnamurthy, N. 2005. Extractive Metallurgy of Rare Earths. London, New York, Washington: CRC Press.

Huang, X.W., Long, Z.Q., Wang, L.S., Feng, Z.Y. 2015. Technology development for rare earth cleaner hydrometallurgy in China. *Rare Metals*, vol. 34, pp. 215–222.

Josso, P., Roberts, S., Teagle, D.A., Pourret, O., Herrington, R., De Leon Albarran, C.P. 2018. Extraction and separation of rare earth elements from hydrothermal metalliferous sediments. *Minerals Engineering*, vol. 118, pp. 106–121.

Judge, W., Azimi, G. 2020. Recent progress in impurity removal during rare earth element processing: A review. *Hydrometallurgy*, vol. 196, 105435.

Judge, W., Ng, K., Moldoveanu, G., Kolliopoulos, G., Papangelakis, V., Azimi, G. 2023. Solubilities of heavy rare earth sulfates in water (gadolinium to lutetium) and H_2SO_4 solutions (dysprosium). *Hydrometallurgy*, vol. 218, 106054.

Kang, H.K., Park, H.C., Kim, K.H. 1995. Crystallite size control of aluminium sulphate precipitated in ethanol from kaolin-derived leach liquor. *Journal of materials science letters*, vol. 14, pp. 1338–1339.

Kaya, Ş., Peters, E.M., Forsberg, K., Dittrich, C., Stopic, S., Friedrich, B. 2018. Scandium recovery from an ammonium fluoride strip liquor by anti-solvent crystallization. *Metals*, vol. 8, p. 767.

Korkmaz, K., Alemrajabi, M., Rasmuson, Å.C., Forsberg, K.M. 2020. Separation of valuable elements from NiMH battery leach liquor via antisolvent precipitation. *Separation and Purification Technology*, vol. 234, 115812.

Ma, C., Gamarra, J. D., Younesi, R., Forsberg, K., Svärd, M. 2023. Antisolvent crystallization from deep eutectic solvent leachates of LiNi1/3Mn1/3Co1/3O_2 for recycling and direct synthesis of battery cathodes. *Resources, Conservation and Recycling*, vol. 198, 107210.

Moldoveanu, G., Kolliopoulos, G., Judge, W., Ng, K., Azimi, G., Papangelakis, V. 2024. Solubilities of individual light rare earth sulfates (lanthanum to europium) in water and H_2SO_4 solutions (neodymium sulfate). *Hydrometallurgy*, vol. 223, 106194.

Nyakairu, G.W., Koeberl, C. 2001. Mineralogical and chemical composition and distribution of rare earth elements in clay-rich sediments from central Uganda. *Geochemical Journal*, vol. 35, pp. 13–28.

OLI Systems Inc 2021. OLI Studio Stream Analyzer, vol. 11. *Morris Plains*, New Jersey.

Pawar, N., Svärd, M., Forsberg, K. 2024. Recovery of Rare Earth Sulfate Hydrates Using Antisolvent Crystallization. TMS Annual Meeting and Exhibition. *Springer*, pp. 55–62.

Ram, R., Becker, M., Brugger, J., Etschmann, B., Burcher-Jones, C., Howard, D., Kooyman, P.J., Petersen, J. 2019. Characterisation of a rare earth element-and zirconium-bearing ion-adsorption clay deposit in Madagascar. *Chemical Geology*, vol. 522, pp. 93–107.

Runde, W., Meinrath, G., Kim, J. 1992. A study of solid-liquid phase equilibria of trivalent lanthanide and actinide ions in carbonate systems. *Radiochimica Acta*, vol. 58, pp. 93–100.

Salim, H., Sahin, O., Elsawah, S., Turan, H., Stewart, R. A. 2022. A critical review on tackling complex rare earth supply security problem. *Resources Policy*, vol. 77, 102697.

Schulze, R., Lartigue-Peyrou, F., Ding, J., Schebek, L., Buchert, M. 2017. Developing a life cycle inventory for rare earth oxides from ion-adsorption deposits: key impacts and further research needs. *Journal of Sustainable Metallurgy*, vol. 3, pp. 753–771.

Silva, R.G., Morais, C.A., Teixeira, L.V., Oliveira, É.D. 2019. Selective precipitation of high-quality rare earth oxalates or carbonates from a purified sulfuric liquor containing soluble impurities. *Mining, Metallurgy & Exploration*, vol. 36, pp. 967–977.

Spahiu, K., Bruno, J. 1995. A selected thermodynamic database for REE to be used in HLNW performance assessment exercises. Swedish Nuclear Fuel and Waste Management Co.

Sussens, J., Chivavava, J., Lewis, A.E. 2024. The recovery of yttrium sulfate through antisolvent crystallization using alcohols. *Separation and Purification Technology*, vol. 346, 127459.

Temga, J.P., Sababa, E., Mamdem, L.E., Bijeck, M.L.N., Azinwi, P.T., Tehna, N., Zame, P. Z.O., Onana, V.L., Nguetnkam, J.P., Bitom, L.D. 2021. Rare earth elements in tropical soils, Cameroon soils (Central Africa). *Geoderma Regional*, vol. 25, e00369.

Wang, M., Huang, X., Feng, Z., Xia, C., Meng, D., Yu, Z. 2021. Behavior of sulfate in preparation of single light rare earth carbonate by Mg $(HCO_3)_2$ precipitation method. *Journal of Rare Earths*, vol. 39, pp. 850–857.

Xiao, Y.F., Feng, Z.Y., Hu, G.H., Huang, L., Huang, X.W., Chen, Y.Y., Li, M.L. 2015. Leaching and mass transfer characteristics of elements from ion-adsorption type rare earth ore. *Rare Metals*, vol. 34, pp. 357–365.

Xiong, Y. 2011. Organic species of lanthanum in natural environments: Implications to mobility of rare earth elements in low temperature environments. *Applied geochemistry*, vol. 26, pp. 1130–1137.

Yin, J.Q., Zou, Z.Q., Tian, J. 2020. Preparation of crystalline rare earth carbonates with large particle size from the lixivium of weathered crust elution-deposited rare earth ores. *International Journal of Minerals, Metallurgy and Materials*, vol. 27, pp. 1482–1488.

Yu, Z., Wang, M., Wang, L., Zhao, L., Feng, Z., Sun, X., Huang, X. 2020. Preparation of crystalline mixed rare earth carbonates by Mg $(HCO_3)_2$ precipitation method. *Journal of Rare Earths*, vol. 38, pp. 292–298.

Zhou, F., Feng, J., Wang, Z., Xu, Y., Zhang, Z., Chi, R. 2017. One step purification of impurities in the leachate of weathered crust elution-deposited rare earth ores. *Physicochemical Problems of Mineral Processing*, vol. 53, no. 2, pp. 1188–1199. ◆